Structural stability of β-beryllium

K. Kádas,[1] L. Vitos,[1,2,3] B. Johansson,[2,3] and J. Kollár[1]
[1]*Research Institute for Solid State Physics and Optics, P.O. Box 49, H-1525 Budapest, Hungary*
[2]*Applied Materials Physics, Department of Materials Science and Engineering, Royal Institute of Technology, SE-10044 Stockholm, Sweden*
[3]*Condensed Matter Theory Group, Department of Physics, Uppsala University, Box 530, SE-751 21 Uppsala, Sweden*
(Received 7 September 2006; revised manuscript received 16 November 2006; published 31 January 2007)

Using density-functional theory formulated within the framework of the exact muffin-tin orbitals method, we investigate the stability of the body-centered-cubic phase of Be (β-Be). The elastic constants and Debye temperature of β-Be are calculated over a wide volume range and compared to those obtained for the low-temperature hexagonal phase (α-Be). A significant difference in the anisotropy of the bcc and hcp structures is found. In line with experiments, we predict that the hcp$\rightarrow$bcc phase transition occurs at 240 GPa at 0 K and 239 GPa at ambient temperature. We find that the cubic shear constant $C'=(C_{11}-C_{12})/2$ rapidly decreases for volumes above $\sim 1.05V_0$, where V_0 is the zero temperature equilibrium volume for β-Be. At $1.17V_0$, the stability condition $C'>0$ is violated and the bcc phase becomes mechanically unstable. We demonstrate that at 0 K, the softening of β-Be near its experimental volume of $1.063V_0$ is related to an electronic topological transition due to the increased number of occupied s states near the Fermi level compared to that at V_0. This softening turns out to be important for the stability of the bcc phase before melting. The disclosed electronic topological transition is found to be present in other analogous hexagonal metals as well.

DOI: 10.1103/PhysRevB.75.035132 PACS number(s): 71.15.Nc, 62.50.+p, 62.20.Dc, 64.70.Kb

I. INTRODUCTION

Beryllium is an important metal for various technological applications. Foils of beryllium being highly transmissive to x rays are commonly applied as x ray windows, whereas bulk beryllium alloys are used as structural materials for high performance aircrafts, spacecrafts, and communication satellites. Alloyed with copper, Be gives a hard, strong, and light alloy with high wear resistance, which is used in computer parts and instruments. It is also important in nuclear reactors as a highly effective moderator and reflector for neutrons. In addition, Be is considered as a good candidate for plasma facing material in fusion reactors.[1]

Under ambient conditions, Be has a hexagonal-closed-packed (hcp) structure[2] and displays several unusual physical properties.[3] It has the lowest Poisson ratio ($\nu=0.05$) among the metals, the lowest crystallographic unit-cell axial ratio of 1.568 among the hexagonal metals $[(c/a)_{ideal}=1.633]$ and has an unusually high Debye temperature (1471 K). Like the early hexagonal transition metals,[4] at high temperature α-Be transforms into the body-centered-cubic (bcc) structure. At zero pressure, β-Be becomes stable only about 30 K before melting at a temperature of 1560 K.

The bulk properties of hcp Be have been extensively studied both theoretically[5–13] and experimentally.[3,14–17] Numerous papers have been devoted to the hcp$\rightarrow$bcc phase transition. Based on linear muffin-tin orbitals (LMTO) calculations, McMahan[18] predicted that the phase transition occurs below 200 GPa at zero temperature. Applying a pseudopotential method, Lam *et al.*[19] found that at $T=0$ K the hcp structure transforms into a bcc or face-centered-cubic (fcc) structure between 100 and 200 GPa. In this calculation, the energy resolution was insufficient to separate the two cubic structures. From calculations based on augmented spherical waves, Meyer-ter-Vehn and Zittel[20] predicted 200 GPa for the transition pressure. Using a scalar relativistic full-potential linear muffin-tin orbital (FP-LMTO) method, Palanivel *et al.*[21] obtained that at zero temperature the bcc structure becomes more stable than the hcp structure above 180 GPa. Based on FP-LMTO calculations, Sin'ko and Smirnov[22] predicted that the hcp$\rightarrow$bcc phase transition occurs at 270 GPa at 300 K. In a recent pseudopotential (PP) calculation, Robert and Sollier[23] obtained 390 GPa for the phase transition at 0 K. On the experimental side, recent measurements failed to find any structural phase transition at ambient temperature and pressures below 200 GPa.[16,17,24,25]

Despite this large number of theoretical studies of the hcp$\rightarrow$bcc phase transition, the number of theoretical investigations of the bcc phase of Be, which could facilitate a deeper understanding of its physical properties and the origin of its dynamical and thermodynamical stability at high temperatures, is very limited.[22,23] In this paper, we address the above problem by using density-functional theory[26,27] formulated within the framework of the exact muffin-tin orbitals (EMTO) method.[28–30] We give a comprehensive account of the elastic properties of Be. The accuracy of our approach is established by comparing the present EMTO results to other theoretical and experimental data. In agreement with the recent FP-LMTO (Ref. 22) and PP (Ref. 23) calculations, we find that at 0 K the bcc phase is mechanically unstable for volumes larger than 1.17 times the equilibrium volume of the bcc phase. Here we propose that the onset of lattice softening in bcc structure happens close to the experimental density and it is connected to an electronic topological transition at the N point from the Brillouin zone. We show that this softening is important for the stability of the bcc phase before melting. Furthermore, we demonstrate that this scenario is present in other hexagonal systems having a high-temperature bcc phase.

The paper is organized as follows. In Sec. II, we briefly review the techniques used in a theoretical determination of

the elastic constants and Debye temperature, and, for completeness, we give the most important numerical details used in the EMTO calculations. The present theoretical results are disclosed and compared to available experimental and theoretical data in the first part of Sec. III. In the second part of this section the electronic origin of the observed anomalous trends is discussed. The paper ends with conclusions.

II. COMPUTATIONAL METHOD

In a body-centered-cubic system there are three independent elastic constants: C_{11}, C_{12}, and C_{44}. They can be obtained by calculating the total energy as a function of small strains δ applied on the parent lattice. In the present application, the two cubic shear constants, $C'=(C_{11}-C_{12})/2$ and C_{44}, have been obtained from volume-conserving orthorhombic and monoclinic distortions, respectively. Details about these distortions can be found in Refs. 31 and 32. We mention that the use of volume conserving deformations allows us to identify the calculated elastic constants with the stress-strain coefficients used for wave propagation velocity.[33–36] In these calculations, at each volume V, the total energy was computed for six different orthorhombic and monoclinic distortions ($\delta_{ort/mon}=0.00, 0.01, \ldots, 0.05$). The bulk modulus B was determined from an exponential Morse-type function[37] fitted to the total energies of the nondistorted bcc structure ($\delta=0$) calculated for ten different volumes. Finally, C_{11} and C_{12} were separated by using C' and the cubic bulk modulus $B=(C_{11}+2C_{12})/3$.

Using the same approach, we have also calculated the elastic constants of α-Be. These data are used to (i) establish the accuracy of our calculations, (ii) parallel the bcc elastic constants with those obtained for the hcp phase, and (iii) estimate the stability field of β-Be. The total energy of hcp Be was calculated for seven different volumes. At each volume V, the theoretical hexagonal axial ratio $(c/a)_0$ was determined by minimizing the total energy $E(V,c/a)$ calculated for nine different c/a ratios close to the energy minimum. The hexagonal bulk modulus was obtained from the Morse function[37] fitted to the energy minima $E(V,(c/a)_0)$. The five hexagonal elastic constants, C_{11}, C_{12}, C_{13}, C_{33}, and C_{44}, were obtained from the bulk modulus, $B=[C_{33}(C_{11}+C_{12})-2C_{13}^2]/C_S$, where $C_S=C_{11}+C_{12}+2C_{33}-4C_{13}$, the logarithmic volume derivative of the hexagonal lattice parameter, *viz.* $d\ln(c/a)_0/d\ln V=-(C_{33}-C_{11}-C_{12}+C_{13})/C_S$, and three isochoric strains, as described in Ref. 33. In the isochoric distortions, the total energy was calculated for six different orthorhombic and monoclinic distortions ($\delta_{ort/mon}=0.00, 0.01, \ldots, 0.05$) for $C_{66}=(C_{11}-C_{12})/2$ and C_{44}, respectively, and for nine hexagonal distortions ($\delta_{hex}=-0.04, -0.03, \ldots, 0.00, \ldots, 0.04$) for C_S.

The anomalously high Debye temperature of Be indicates that phonon vibrations might play an important role already at ambient temperature. We make use of the Debye model to account for the main lattice vibration effects. The present approach is similar to that from Ref. 38. From the elastic constants, we have determined the volume dependent Debye sound velocity $v_D(V)$ and ultimately the Debye temperature[39]

$$\Theta_D(V)=\frac{\hbar}{k_B}\left(\frac{6\pi^2}{V}\right)^{1/3}v_D(V), \tag{1}$$

where $\hbar$ and k_B are the Planck and Boltzmann constants, respectively. This volume dependent Debye temperature has been used in the conventional Debye model to find the Helmholtz free energy

$$F(V,T)=E(V)-k_BT\left(\frac{3}{(\Theta_D/T)^3}\int_0^{\Theta_D/T}\frac{y^3}{e^y-1}dy - 3\ln(1-e^{-\Theta_D/T})\right)+\frac{9}{8}k_B\Theta_D, \tag{2}$$

where $E(V)$ denotes the electronic energy obtained from an EMTO calculation carried out at zero temperature and the last term from the right-hand side is the zero-point motion. In this expression the electronic entropy has been omitted. Finally, the Gibbs energy has been calculated from the free energy as $G(P,T)=F(V,T)+PV$, where $P=-\partial E(V)/\partial V$ is the pressure.

The present *ab initio* calculations are based on the density-functional theory (DFT) (Ref. 26) using the generalized gradient approximation (GGA) (Ref. 40) for the exchange-correlation functional. This approximation proved to be slightly more accurate in the case of hcp Be than the local-density approximation.[11] The Kohn-Sham equations[27] were solved using the exact muffin-tin orbitals method.[28–30] In the self-consistent calculations, the one-electron equations were treated within the scalar relativistic and soft core approximations. The EMTO Green's function was calculated for 32 energy points. In the case of strained bcc structures $\sim 10^5 k$ points were used in the irreducible part of the orthorhombic Brillouin zones. A similar k-point density was ensured in the case of the hcp and strained hcp structure as well. The total charge density was expanded in spherical harmonics, including terms up to $l_{max}=10$.

III. RESULTS AND DISCUSSION

A. Elastic properties of Be

We establish the accuracy of our method by comparing the present theoretical bulk properties of Be with the available experimental data.[3,14,41] Since no measurements have been published for the elastic properties of bcc Be, in this comparison we consider only the hcp phase. In Table I, we list the EMTO equilibrium hcp volume V_0 and the corresponding equilibrium bulk modulus B_0, hexagonal lattice parameter $(c/a)_0$, hexagonal elastic constants C_{ij}^0 and Debye temperature Θ_D^0 calculated at $T_0=0$ K. Since the experimental data shown in the last column of Table I refer to the room temperature T_r, we have determined the room temperature V_0 and B_0 as well. We find that these two parameters are in excellent agreement with the experimental values. The present room-temperature bulk modulus, for instance, differs by 4.4% and 1.7% from the values reported by Migliori *et al.*[3] and by Rowland and White,[14] respectively. This good correspondence also means that the thermal expansion in hcp Be is properly accounted for within the present Debye

TABLE I. Calculated and experimental equilibrium (zero pressure) bulk properties of hcp Be. V_0 is the volume [in units of $(\mathrm{a.u.})^3$/atom], B_0 the bulk modulus (GPa), $(c/a)_0$ the hexagonal lattice parameter, C_{ij}^0 are the hexagonal elastic constants (GPa), and Θ_D^0 is the Debye temperature calculated from the elastic constants (K). In calculations at T_0=0 no zero-point vibrations [last term in Eq. (2)] were taken into account. T_r denotes the room temperature. In full-potential linear muffin-tin orbital (FP-LMTO) (Ref. 22) and pseudopotential (PP) (Ref. 23) calculations the quoted data at T_0 (except the FP-LMTO V_0 and B_0) were obtained at the experimental volume.

	EMTO		FP-LMTO		PP	Experiment
	T_0	T_r	T_0	T_r	T_0	T_r
V_0	53.45	54.63	53.46	54.44		54.78 (Ref. 41)
B_0	118.8	111.7	122	114	114.5	116.8 (Ref. 3), 109.8 (Ref. 14)
$(c/a)_0$	1.578		1.573		1.570	1.568 (Ref. 3)
C_{11}^0	304.81		300.8		305.9	293.6 (Ref. 3)
C_{12}^0	31.89		14.1		18.8	26.8 (Ref. 3)
C_{13}^0	3.59		7.1		10.4	14.0 (Ref. 3)
C_{33}^0	387.06		359.5		329	356.7 (Ref. 3)
C_{44}^0	163.23		160.2		159.3	162.2 (Ref. 3)
Θ_D^0	1471.2		1465.9		1475	1471 (Ref. 3)

model. Comparing the EMTO hexagonal axial ratio, elastic constants, and Debye temperature obtained at T_0 with the room-temperature experimental data, for the mean absolute value of the relative deviation we obtain ~15%. Part of this error may be ascribed to the volume effect and the rest to the main approximations within the DFT-GGA theory.

In Table I, we also compare our results with earlier theoretical values obtained using a full-potential linear muffin-tin orbitals (FP-LMTO) method[22] and a pseudopotential (PP) method.[23] Associating the numerical error, due to the approximations present in such calculations, with the difference between the FP-LMTO and PP data, the difference between the three sets of theoretical results from Table I can be considered to be reasonable. Regarding the volume dependence of the elastic constants, in Fig. 1 we compare the present hcp elastic constants calculated at seven different volumes with those obtained using the FP-LMTO method.[22] We find that the two sets of elastic constants are in a very good agreement. Therefore we conclude that our *ab initio* approach is suitable for an accurate description of the bulk properties of Be.

The present equilibrium bulk properties of bcc Be are listed in Table II along with two other sets of theoretical results.[22,23] The apparent deviation between the EMTO elastic parameters and earlier results is due to the fact that the quoted FP-LMTO and PP values were obtained at the experimental volume of hcp Be, whereas in the EMTO calculations the T_0=0-K equilibrium volume of bcc Be was used. This latter is ~1.3% smaller than that of the hcp phase at 0 K, ~3.7% smaller than the room-temperature experimental volume of α-Be, and ~5.9% smaller than the experimental volume of β-Be measured between 1523 and 1553 K.[42] The

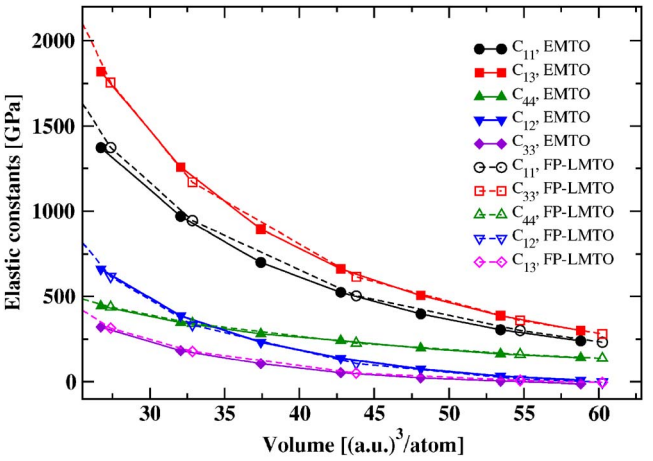

FIG. 1. (Color online) Elastic constants of hcp Be at different volumes. Filled symbols connected by solid lines represent the EMTO results, while open symbols connected with dashed lines are those obtained using the FP-LMTO method (Ref. 22).

denser bcc lattice at 0 K is in line with the experimentally observed volume collapse at the hcp→bcc phase transition.[2] On the other hand, the room-temperature volumes in the bcc and hcp phases are already very close. Taking into account that the present theoretical room-temperature volume of α-Be is close to the experimental value (Table I), this result indicates that the lattice expansion in the bcc phase is overestimated by the Debye model. This finding signals the failure of the Debye model for the bcc phase.

The present elastic constants of bcc Be calculated at T_0 for ten different volumes, corresponding approximately to pressures between −15 and ~270 GPa, are listed in Table III and compared to the FP-LMTO results[22] in Fig. 2. A reasonable agreement between the two sets of data is found. In particular, both in the EMTO and FP-LMTO calculations, the $C_{11}(V)$ and $C_{44}(V)$ curves cross near V=42–45 $(\mathrm{a.u.})^3$. The tetragonal shear constant $C'=(C_{11}-C_{12})/2$ is plotted in the inset of Fig. 2. We find that C' exhibits a normal decreasing behavior up to $V\approx 1.05V_0$, but thereafter it abruptly changes its trend. We observe that this change takes place close to the experimental volume $1.063V_0$ of bcc Be.[42] Above this volume, the bcc phase rapidly loses its mechanical stability. At a

TABLE II. Bulk properties of bcc Be calculated at zero pressure. For notations and units see caption for Table I. The full-potential linear muffin-tin orbital (FP-LMTO) (Ref. 22) and pseudopotential (PP) (Ref. 23) calculations were carried out at the experimental volume of hcp Be [54.78 $(\mathrm{a.u.})^3$/atom].

	EMTO		FP-LMTO	PP
	T_0	T_r	T_0	T_0
V_0	52.78	54.21		
B_0	121.3	110.9	109.5	112.8
C_{11}^0	181.11		146.8	143.7
C_{12}^0	91.41		90.8	96.0
C_{44}^0	224.90		185.2	150.5
Θ_D^0	1216.9		1044.6	962

TABLE III. Theoretical elastic constants of bcc Be (in GPa) calculated at zero temperature as functions of volume. V_0 stands for the optimized volume of the bcc lattice. A_Z and A_E are the Zener and Every anisotropy ratios, respectively.

V/V_0	C_{11}	C_{12}	C_{44}	B	A_Z	$1/A_E$
0.50	1070.07	668.97	773.72	802.67	3.86	−0.26
0.60	714.45	433.81	567.88	527.36	4.05	−0.17
0.70	493.18	289.98	431.11	357.71	4.24	−0.09
0.80	346.76	197.92	336.72	247.53	4.52	−0.02
0.90	252.14	133.59	261.93	173.11	4.42	0.02
1.00	181.11	91.41	224.90	121.31	5.01	0.12
1.05	159.07	72.48	185.47	101.34	4.28	0.09
1.10	136.29	58.46	136.88	84.40	3.52	0.00
1.13	109.94	58.23	109.38	75.47	4.23	0.00
1.16	78.83	61.59	81.48	67.34	9.45	0.02

critical volume of $V_{cr}=1.17V_0$ the tetragonal shear modulus reaches zero and the bcc phase becomes mechanically unstable. At this point, one of the stability requirements for cubic structures, namely $C_{11}>|C_{12}|$, is broken, but the other two stability criteria, $C_{11}+2C_{12}>0$ and $C_{44}>0$, remain valid over the whole volume region considered. Our calculated V_{cr} is in excellent agreement with $1.179V_0$ obtained in the PP study by Robert and Sollier.[23] We note that the calculated behavior of C' between ~50 and ~65 $(\mathrm{a.u.})^3$/atom (inset of Fig. 2) is far too complex to follow a simple analytic form proposed, e.g., in Ref. 43.

The elastic anisotropy of cubic lattices may be characterized by the Zener anisotropy parameter, $A_Z=2C_{44}/(C_{11}-C_{12})$. For an isotropic crystal $A_Z=1$. Our calculated A_Z parameters are given in Table III. They are more than 3.5 times larger than the isotropic limit at every volume, indicating that the bcc phase of Be is very anisotropic. A more natural parameter to use as a measure of the anisotropy in cubic

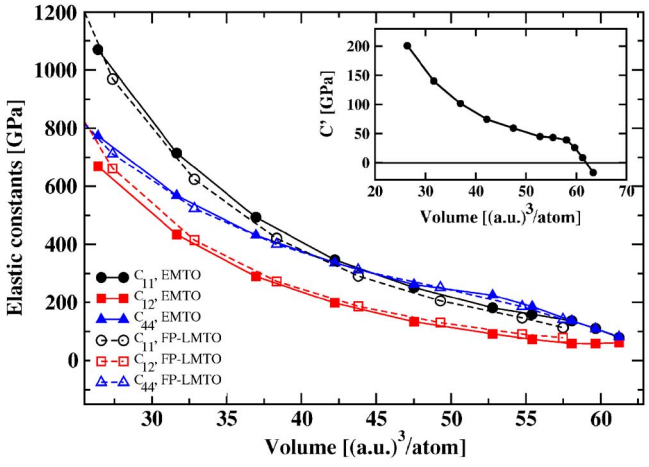

FIG. 2. (Color online) Elastic constants of bcc Be at different volumes. Filled symbols connected by solid lines represent the EMTO results, while open symbols connected with dashed lines are those obtained using the FP-LMTO method (Ref. 22). In the inset, the present C' is shown as a function of volume.

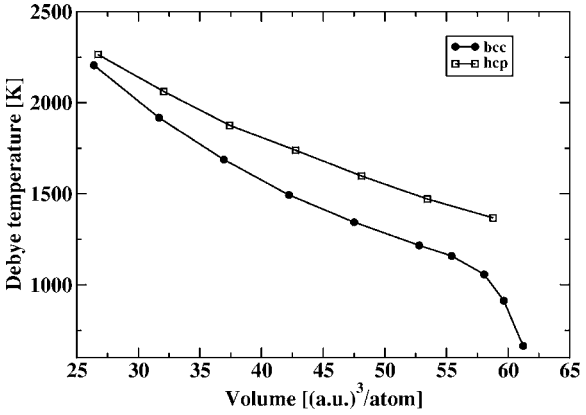

FIG. 3. Theoretical Debye temperatures of bcc (filled circles) and hcp (open squares) Be as functions of volume.

lattices[39] is the Every ratio[44] introduced as $A_E=(C_{11}-C_{12}-2C_{44})/(C_{11}-C_{44})$. For an isotropic system $A_E=0$. The inverse of the Every ratio is given in the last column of Table III. The very small values of $1/A_E$ confirm the strong anisotropy of the bcc Be. Moreover, the Every ratio provides an additional information about the bcc phase. Near 0.84 and $1.11V_0$, where $1/A_E\approx 0$, the sound velocities of the longitudinal and transverse modes are equal in the [100] direction.

The hcp phase is calculated to be mechanically stable over the whole volume interval, since the stability requirements[39] $C_{11}>|C_{12}|$, $C_{33}(C_{11}+C_{12})>2C_{13}^2$, $C_{11}C_{33}>C_{13}^2$, and $C_{44}>0$ are fulfilled for any V. The elastic anisotropy of an hcp lattice may be measured by the compressional wave anisotropy $A_P=C_{33}/C_{11}$ and the two shear wave anisotropy parameters $A_{S1}=(C_{11}+C_{33}-2C_{13})/4C_{44}$, and $A_{S2}=2C_{44}/(C_{11}-C_{12})$. For an isotropic system $A_P=A_{S1}=A_{S2}=1$. Using the elastic constants from Table I, we obtained $A_P=1.27$, $A_{S1}=1.05$, and $A_{S2}=1.20$. According to our results[45] (not shown) and former theoretical data,[22,23] these ratios exhibit a very weak volume dependence, indicating that, in contrast to bcc Be, the anisotropy of hcp Be remains nearly constant with increasing pressure.

In order to compare the elastic anisotropy of the hcp and bcc phases, we use the polycrystalline anisotropy ratio,[39,46] $A_{VR}=(G_V-G_R)/(G_V+G_R)$. Here G_V and G_R are the Voigt (upper) and Reuss (lower) bounds of the shear modulus, respectively. We obtain that the A_{VR} ratio for the hcp phase is always below 0.03, confirming the almost isotropic character of hcp Be. On the other hand, the A_{VR} ratio for the bcc phase varies between 0.18 and 0.48 as a function of volume, and follows the same behavior with volume as A_Z. This significant difference in the anisotropy between the two phases of Be might be used in experiments to detect the structural phase transition, e.g., at high pressure.

The calculated Debye temperatures for α- and β-Be are shown in Fig. 3 as functions of volume. Their equilibrium values are given in Tables I and II. Note the very good agreement between the present $\Theta_{D,hcp}^0$ and the recently published result by Migliori *et al.*[3] In the whole volume range, we have $\Theta_{D,bcc}<\Theta_{D,hcp}$, i.e., the bcc phase is considerably softer than the hcp phase. The difference between $\Theta_{D,bcc}$ and $\Theta_{D,hcp}$ increases with volume. The sharp decrease of the $\Theta_{D,bcc}$

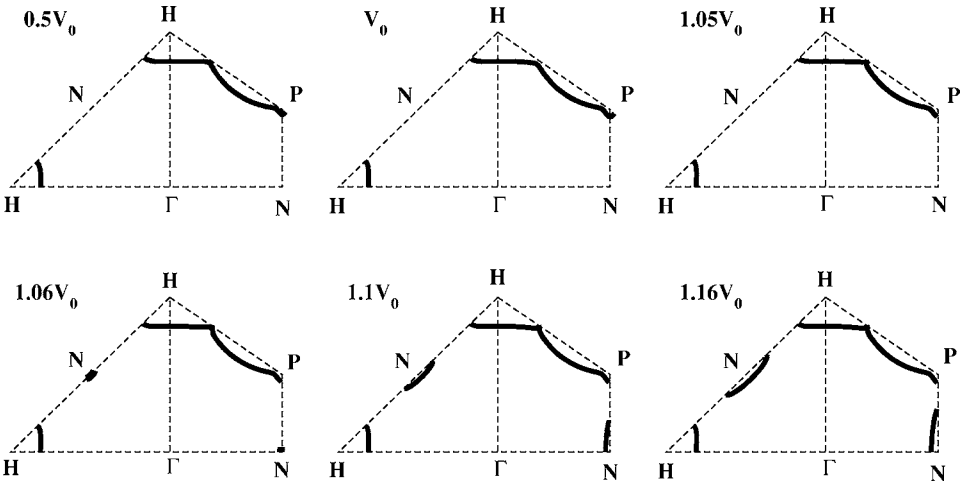

FIG. 4. The (100) and (110) cross sections of the Fermi surface of the bcc Be at four different volumes (V_0 stands for the equilibrium volume of the bcc lattice) as calculated using the EMTO method. Boundaries of the Brillouin zone are denoted by dashed lines. Γ, N, P, and H represent the high-symmetry points of the Brillouin zone.

above ~ 55 (a.u.)^3/atom is a consequence of the loss of mechanical stability marked by the change in the slope of C' in the same region (Fig. 2). We note that the Debye temperature, derived from the elastic constants according to Eq. (1), goes to zero as one approaches the critical volume V_{cr}, but it is not defined for a lattice with $C' < 0$.

Calculating the hcp and bcc Gibbs free energies, we can determine the pressure and temperature where the bcc phase becomes stable relative to the hcp phase. At zero temperature and zero pressure, the hcp phase is calculated to be more stable than the bcc one, with a bcc-hcp energy difference of 6.22 mRy/atom. In line with recent experiments[16,17,24,25] and in good agreement with a FP-LMTO calculation by Sin'ko and Smirnov,[22] we obtain that at T_0 the bcc phase becomes stable above $P_{tr}(T_0)=240$ GPa. Upon this phase transition, the atomic volume changes from 27.59 to 27.36 (a.u.)^3/atom. Since around this pressure the hcp and bcc Debye temperatures are close to each other (Fig. 3), at low temperatures the transition pressure is expected to be decreased only slightly by the phonon contributions. Indeed, at room temperature we obtain $P_{tr}(T_r)=239$ GPa.

B. Instability of the bcc phase

In order to provide an explanation for the obtained softening of the bcc phase at low temperatures and near the experimental density of β-Be, we examine its electronic structure and search for possible anomalies between V_0 and $1.1V_0$. Figure 4 displays two cross sections of the Fermi surface of bcc Be calculated at six different volumes $0.5V_0$, V_0, $1.05V_0$, $1.06V_0$, $1.1V_0$, and $1.16V_0$. At volumes $\leq 1.05V_0$ (upper panels in Fig. 4), the Fermi surface topology remains unchanged with increasing volume. However, for $1.06V_0$ a new electron pocket appears around the N point, and it becomes larger with increasing volume (lower panels in Fig. 4).

The pocket appears because some unoccupied bands, situated above the N point at the equilibrium volume, are crossed by the Fermi level at larger volumes. This can be seen in the left panels of Fig. 5, where the total and partial density of states (DOS) of bcc Be are shown for V_0 and $1.16V_0$. At V_0 (upper left panel), there are pronounced s and d peaks situated slightly above the Fermi level (E_F). With increasing volume (lower left panel), these peaks move down below E_F

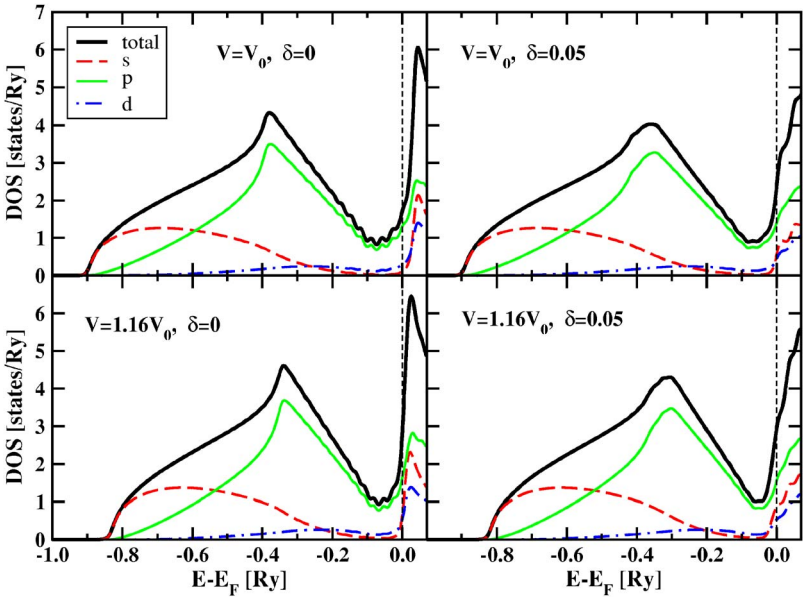

FIG. 5. (Color online) Density of states of bcc Be at the equilibrium volume V_0 (upper panels), and at $1.16V_0$ (lower panels). DOS for the nondistorted bcc structures are shown in the left panels ($\delta_{ort}=0$), while the right panels display the DOS for the structures distorted by the orthorhombic strain ($\delta_{ort}=0.05$) used to compute C'. Total DOS curves are represented by solid thick lines, partial s-, p-, and d-DOS curves are denoted by thin dashed, solid, and dot dashed lines, respectively. Vertical dashed lines show the Fermi level (E_F).

and, as a consequence, the number of states at E_F increases. We have found that this increase arises mainly from the variation of the number of *s* states. The volume induced shift of the originally unoccupied *s* states towards energies below the Fermi level is a result of the altered *sp* hybridization. To illustrate this, we quantify the *sp* hybridization by the total number of *s* and *p* states. From the present results we obtain that, when the volume of bcc Be increases from V_0 to $1.16V_0$, the number of *s* electrons increases by ~ 0.03 and the number of *p* electrons decreases by the same amount (the number of *d* electrons remains practically unchanged).

Based on the information from Fig. 4 and taking into account the numerical errors of our calculations estimated using different Brillouin-zone samplings, we predict that in bcc Be an electronic topological transition (ETT) occurs at $(1.06 \pm 0.005)V_0$. Within the error limits, this volume coincides with the one where C' starts to deviate from a normal trend (Fig. 2), which in fact it is very close to the experimental volume of bcc Be.[42] Therefore we associate the ETT with the softening (decreasing C') of the bcc lattice with increasing volume. Below we expand on the arguments that support this.

The effect of lattice distortion associated with the shear modulus C' on the *s* peak above the Fermi level is demonstrated in Fig. 5. In the left panels, we show the total and partial DOS for an orthorhombic ($\delta_{ort}=0.05$) lattice used in the numerical determination of C'. We can see that at constant volume the lattice distortion shifts the unoccupied *s* peak towards the Fermi level. This gives a negative contribution to the energy change upon lattice distortion and thus decreases the shear elastic constant C'. In fact, already at volumes slightly below the volume where the ETT occurs in an undistorted bcc lattice, these *s* states give a negative contribution to C'. However, because of the rapid increase of the density of states above the Fermi level, the softening effect becomes pronounced at $\sim 1.06V_0$, where the *s* states at the *N* point reach the Fermi level. At this (or a larger) volume a significant amount of *s* states are pushed below the Fermi level upon infinitesimal small lattice distortion. We conclude that in β-Be, the *s* states centered around the *N* point rapidly soften C' with increasing volume, for $V \gtrsim 1.06V_0$. We would like to point out that in accordance with former observations,[47,48] we have found that the sharpness of the transition in C' and also the position of the ETT depend very sensitively on the numerical details, such as the complex energy integration, the Brillouin-zone sampling, smearing of the electronic states, or the size of the distortion δ_{ort} used in the calculation of the shear constant C'.

The disclosed ETT may be connected to the appearance of the imaginary phonon frequencies in bcc Be. Because the present method does not allow us to compute the phonon spectra, we have to rely on the previous pseudopotential results by Robert and Sollier.[23] In the PP study, the frequency of *N*-point phonons in β-Be was calculated to be imaginary at large volumes. It was obtained that this phonon mode becomes unstable already at a volume which is well below $1.06V_0$. We attribute this to the smearing applied on the electronic states. In an *ab initio* simulation using a smearing technique, e.g., the one employed in Ref. 23, the effect of the *s* peak (Fig. 5) is estimated to show up already at volumes where this peak is still above E_F, i.e., at volumes below $1.06V_0$. We suggest that in bcc Be, the *N*-point phonons become imaginary close to the volume where the ETT occurs. However, in order to give a more clear evidence for this, further theoretical investigations are necessary.

In connection with the softening of the bcc lattice, we comment on the hcp $\rightarrow$ bcc phase transition at ambient pressure. Comparing the hcp and bcc Gibbs energies at zero pressure, we obtain that the phase transition takes place at ~ 1381 K. This temperature is smaller than the one observed in experiments (1530 K). Furthermore, near the transition temperature, the calculated bcc atomic volume of 57.44 $(\mathrm{a.u.})^3$/atom (corresponding to $\sim 1.09V_0$) is larger than 56.52 $(\mathrm{a.u.})^3$/atom obtained for the hcp phase. This 1.6% increase of the atomic volume is in contrast to observations.[2] Note that the calculated bcc transition volume is $\sim 3\%$ larger than the experimental value.[42] This error should be contrasted, e.g., with the 0.3% difference obtained between the calculated and measured room-temperature atomic volumes for hcp Be (Table I). The above discrepancy for the transition temperature may partly be due to the Debye model but also to the presence of the imaginary phonons in the bcc phase. We should keep in mind that in this estimation, for the Debye temperature [Eq. (1)], we used the 0-K elastic constants. Since the bcc phase becomes unstable with increasing volume,[23] the theoretical Debye temperature calculated from the elastic constants is expected to be underestimated. The same is true in the case of a Debye temperature obtained from the moment frequencies calculated from the 0-K phonon spectra containing imaginary modes. Strictly speaking, for volumes where β-Be is dynamically unstable, neither the Debye temperature nor the Gibbs energy is defined for the this phase.[39] As a matter of fact, with increasing temperature the imaginary phonon modes near the *N* point[23] should be stabilized by lattice vibrations. This would increase the Debye temperature derived either from the temperature-dependent elastic constants or phonon spectra and thus would lead to a higher hcp $\rightarrow$ bcc transition temperature. In this context, the underestimation of the hcp $\rightarrow$ bcc transition temperature and overestimation of the lattice expansion in the bcc phase by a Debye model based on 0-K parameters seems most plausible.

One may ask the question whether the above electronic topological transition is relevant for the phase transition in Be. To answer this, we estimate how the tetragonal shear modulus C' of bcc Be would behave in the absence of the ETT. Using an analytic form proposed in Ref. 43, we extrapolate the calculated elastic constants for $V \leq V_0$ (inset of Fig. 2) to volumes above V_0. The new bcc Debye temperatures, calculated from the extrapolated bcc C' elastic constants, increase the hcp $\rightarrow$ bcc transition temperature at zero pressure by more than 100 K. We recall that the experimental stability field of β-Be at ambient pressure is only 30 K. This clearly indicates that the bcc phase of Be could not be stabilized at high temperatures without the C' softening caused by the ETT at the *N* point.

In order to show that the revealed mechanism behind the softening of the bcc phase is not specific only to Be, we consider some analogous systems. Among the elemental metals and metallic alloys, the Hume-Rothery alloys in their

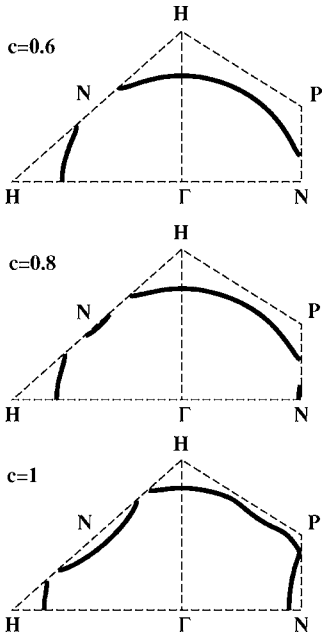

FIG. 6. The Fermi surface of bcc Ag-Zn alloys as a function of chemical composition. c denotes the atomic fraction of Zn. For notations see caption for Fig. 4.

ϵ phase[49] crystallize in a hcp structure with unusually low $(c/a)_0$. Here we focus on the $Ag_{1-c}Zn_c$ alloys with $0.68<c<0.87$. These alloys possess a hcp crystal structure with $(c/a)_0=1.56-1.58$. Recently, Magyari-Köpe *et al.*[32,50] calculated the elastic constants of Ag-Zn alloys both in the hcp and bcc structures. They have found that, while the hcp phase of Zn-rich Ag-Zn alloys is mechanically stable for any composition, in the bcc phase C' becomes zero at $c\approx 0.8$ and remains negative with increasing Zn concentrations (see Fig. 5 from Ref. 32). In Fig. 6, we show the calculated Fermi surfaces for Ag-Zn alloys at three different concentrations. Interestingly, one can observe a similar electronic topological transition in Ag-Zn as the one in bcc Be. A pocket centered at the N point develops for $c\gtrsim 0.8$. As c changes from 0.6 to 0.8, the number of s electrons of Ag and Zn atoms increases from 1.07 to 1.09 and from 0.73 to 0.75, respectively. Like in the case of bcc Be, the s states around the N point start to fill up in the region where the system becomes mechanically unstable. But in contrast to Be, in Ag-Zn alloys the change in the s occupation number is driven by alloying rather than by the reduced sp hybridization with increasing volume.

Phonon instabilities near the N point have also been observed in early hexagonal transition metals (e.g., Sc, Ti, Zn, La, Hf).[4] These elements have a hcp crystal structure at ambient temperature and bcc structure at high temperature. It is very likely that part of the lattice instability in the bcc phase of these metals is also due to the N-point electron pocket discussed above. We can recall other examples that might support this scenario. For instance, the Ti-rich Ti-Mo and Ti-Cr alloys have a high-temperature bcc phase and a stable hcp phase at ambient temperature. The Debye temperature of the bcc phase decreases sharply with increasing Ti concentration, at about 15% Mo and 10% Cr in Ti-Mo and Ti-Cr, respectively.[51] In Ti-Cr, C' decreases with decreasing Cr concentration, and becomes zero at about 5% Cr. However, revealing the electronic origin of these phenomena necessitates further theoretical investigations.

IV. CONCLUSIONS

We have calculated the lattice parameters, elastic constants, and Debye temperatures of hcp and bcc Be as functions of volume. The hcp phase is found to remain mechanically stable and nearly isotropic over the whole volume range considered. In the bcc phase, the tetragonal shear constant C' sharply decreases for a volume above $\sim 1.05V_0$, where the bcc phase rapidly loses its mechanical stability and becomes unstable at $1.17V_0$. In contrast to the hcp phase, bcc Be turns out to be extremely anisotropic. We suggest that this remarkable difference may be used in experiments to detect the high-pressure hcp$\rightarrow$bcc structural phase transition. In line with a few previous calculations, we have found that at 0 K the hcp$\rightarrow$bcc phase transition occurs at $\sim$240 GPa. Furthermore, at temperatures up to a few hundred K, entropy plays only a minor role in the transition pressure.

The soft C' mode in bcc Be is reflected in a significantly smaller Debye temperature compared to the one obtained for the hcp phase. At ambient pressure, this difference is large enough to stabilize the bcc phase before melting. However, the sharp decrease in C' above $\sim 1.05V_0$ is associated with a sharp decrease of the bcc Debye temperature. This indicates that, due to the instability of the bcc phase at large volumes, the theoretical Debye temperature calculated from the 0-K elastic constants (or eventually phonon spectra) and thus the actual hcp$\rightarrow$bcc transition temperature should be underestimated. To overcome this problem, molecular-dynamics simulations are needed, which can account for the stabilization of the imaginary phonon modes with increasing temperature.

We have shown that the lattice softening of the bcc phase near and below its experimental density appears as a result of an sp hybridization driven electronic topological transition at the N point from the Brillouin zone. We have found that this softening is responsible for the stability of the bcc phase before melting. A clear analogy between Be and the $Ag_{1-c}Zn_c$ alloys with $0.68<c<0.87$ has been found. This analogy concerns, first of all, the low-temperature crystal structure and hexagonal lattice parameter, and the mechanism behind the dynamical stability and instability of the bcc phase.

ACKNOWLEDGMENTS

This work was supported by Hungarian Scientific Research Fund: research project OTKA T046773 and T048827. The calculations were done at the Hungarian National Supercomputer Center. L.V. and B.J. also acknowledge financial support from the Swedish Research Council and the Swedish Foundation for Strategic Research.

[1] K. L. Wilson, R. A Causey, W. L. Hsu, B. E. Mills, M. F. Smith, and J. B. Whitley, J. Vac. Sci. Technol. A **8**, 1750 (1990).
[2] D. A. Young, *Phase Diagrams of the Elements* (University of California Press, Berkeley, CA, 1991).
[3] A. Migliori, H. Ledbetter, D. J. Thoma, and T. W. Darling, J. Appl. Phys. **95**, 2436 (2004).
[4] K. Persson, M. Ekman, and V. Ozoliņš, Phys. Rev. B **61**, 11221 (2000).
[5] F. Perrot, Phys. Rev. B **21**, 3167 (1980).
[6] R. Dovesi, C. Pisani, F. Ricca, and C. Roetti, Phys. Rev. B **25**, 3731 (1982).
[7] M. Y. Chou, P. K. Lam, and M. L. Cohen, Solid State Commun. **42**, 861 (1982).
[8] M. Y. Chou, P. K. Lam, and M. L. Cohen, Phys. Rev. B **28**, 1696 (1983).
[9] M. Y. Chou, P. K. Lam, and M. L. Cohen, Phys. Rev. B **28**, 4179 (1983).
[10] P. Blaha and K. Schwarz, J. Phys. F: Met. Phys. **17**, 899 (1987).
[11] N. A. W. Holzwarth and Y. Zeng, Phys. Rev. B **51**, 13653 (1995).
[12] U. Häussermann and S. I. Simak, Phys. Rev. B **64**, 245114 (2001).
[13] G. K. H. Madsen, P. Blaha, and K. Schwarz, J. Chem. Phys. **117**, 8030 (2002).
[14] W. D. Rowland and J. S. White, J. Phys. F: Met. Phys. **2**, 231 (1972).
[15] A. T. Dinsdale, CALPHAD: Comput. Coupling Phase Diagrams Thermochem. **15**, 317 (1991).
[16] H. Olijnyk and A. P. Jephcoat, J. Phys.: Condens. Matter **12**, 8913 (2000).
[17] N. Velisavljevic, G. N. Chestnut, Y. K. Vohra, S. T. Weir, V. Malba, and J. Akella, Phys. Rev. B **65**, 172107 (2002).
[18] A. K. McMahan, in *Shock Waves in Condensed Matter - 1981*, edited by W. J. Nellis, L. Seaman, and R. A. Graham, AIP Conf. Proc. No. 78 (AIP, New York, 1982), p. 340.
[19] P. K. Lam, M. Y. Chou, and M. L. Cohen, J. Phys. C **17**, 2065 (1984).
[20] J. Meyer-ter-Vehn and W. Zittel, Phys. Rev. B **37**, 8674 (1988).
[21] B. Palanivel, R. S. Rao, B. K. Godwal, and S. K. Sikka, J. Phys.: Condens. Matter **12**, 8831 (2000).
[22] G. V. Sin'ko and N. A. Smirnov, Phys. Rev. B **71**, 214108 (2005).
[23] G. Robert and A. Sollier, J. Phys. IV **134**, 257 (2006).
[24] K. Nakano, Y. Akahama, and H. Kawamura, J. Phys.: Condens. Matter **14**, 10569 (2002).
[25] W. J. Evans, M. J. Lipp, H. Cynn, C. S. Yoo, M. Somayazulu, D. Häusermann, G. Shen, and V. Prakapenka, Phys. Rev. B **72**, 094113 (2005).
[26] P. Hohenberg and W. Kohn, Phys. Rev. **136B**, 864 (1964).
[27] W. Kohn and L. J. Sham, Phys. Rev. **140A**, 1133 (1965).
[28] L. Vitos, H. L. Skriver, B. Johansson, and J. Kollár, Comput. Mater. Sci. **18**, 24 (2000).
[29] L. Vitos, Phys. Rev. B **64**, 014107 (2001).
[30] O. K. Andersen, O. Jepsen, and G. Krier, in *Lectures on Methods of Electronic Structure Calculation* (World Scientific, Singapore, 1994), p. 63.
[31] A. Taga, L. Vitos, B. Johansson, and G. Grimvall, Phys. Rev. B **71**, 014201 (2005).
[32] B. Magyari-Köpe, G. Grimvall, and L. Vitos, Phys. Rev. B **66**, 064210 (2002); **66**, 179902 (2002).
[33] G. Steinle-Neumann, L. Stixrude, and R. E. Cohen, Phys. Rev. B **60**, 791 (1999).
[34] P. M. Marcus, H. Ma, and S. L. Qiu, J. Phys.: Condens. Matter **14**, L525 (2002).
[35] P. M. Marcus and S. L. Qiu, J. Phys.: Condens. Matter **16**, 8787 (2004).
[36] G. Steinle-Neumann and R. E. Cohen, J. Phys.: Condens. Matter **16**, 8783 (2004).
[37] V. L. Moruzzi, J. F. Janak, and K. Schwarz, Phys. Rev. B **37**, 790 (1988).
[38] G. V. Sin'ko and N. A. Smirnov, J. Phys.: Condens. Matter **14**, 6989 (2002).
[39] G. Grimvall, *Thermophysical Properties of Materials*, enlarged and revised edition (North-Holland, Amsterdam, 1999).
[40] J. P. Perdew, K. Burke, and M. Ernzerhof, Phys. Rev. Lett. **77**, 3865 (1996).
[41] K. J. H. Mackay and N. A. Hill, J. Nucl. Mater. **8**, 263 (1963).
[42] P. Villars and L. D. Calvert, *Pearson's Handbook of Crystallographic Data for Intermetallic Phases* (American Society for Metals, Metals Park, OH, 1989), Vol. 2.
[43] L. Burakovsky, C. W. Greeff, and D. L. Preston, Phys. Rev. B **67**, 094107 (2003).
[44] A. G. Every, Phys. Rev. B **22**, 1746 (1980).
[45] K. Kádas, L. Vitos, and J. Kollár (unpublished).
[46] D. H. Chung and W. R. Buessem, J. Appl. Phys. **38**, 2010 (1967).
[47] G. Steinle-Neumann, L. Stixrude, and R. E. Cohen, Phys. Rev. B **63**, 054103 (2001).
[48] G. V. Sin'ko and N. A. Smirnov, J. Phys.: Condens. Matter **17**, 559 (2005).
[49] T. B. Massalski, J. Phys. Radium **23**, 647 (1962).
[50] B. Magyari-Köpe, L. Vitos, and G. Grimvall, Phys. Rev. B **70**, 052102(4) (2004).
[51] E. W. Collings, J. C. Ho, and R. I. Jaffee, Phys. Rev. B **5**, 4435 (1972).